JOURNAL OF BACTERIOLOGY, Feb. 1996, p. 705–713 Vol. 178, No. 3
0021-9193/96/$04.00+0

Transcriptional Regulation of the *Bacillus subtilis menp1* Promoter

XUAN QIN AND HARRY W. TABER*

Wadsworth Center, New York State Department of Health, and Department of Biomedical Sciences, School of Public Health, State University of New York at Albany, Albany, New York 12201-2002

Received 6 September 1995/Accepted 20 November 1995

The *Bacillus subtilis men* genes encode biosynthetic enzymes for formation of the respiratory chain component menaquinone. The *menp1* promoter previously was shown to be the primary *cis* element for *menFD* gene expression. In the present work, it was found that either supplementation with nonfermentable carbon sources or reutilization of glycolytic end products increased *menp1* activity in the late postexponential phase. The effect on *menp1* activity by a particular end product (such as acetoin or acetate) was prevented by blocking the corresponding pathway for end product utilization. Alteration of a TGAAA motif within the promoter region resulted in unregulated *menp1* activity throughout the culture cycle, irrespective of the carbon source added.

Menaquinone (MK) is a lipophilic nonprotein component of the *Bacillus subtilis* respiratory chain (Fig. 1B) essential for growth and viability. Not only does MK participate in redox reactions of oxidative respiration, but it also plays a crucial role in maintenance of an electrochemical membrane potential and regulation of cytochrome formation (5, 6, 34). MK is also necessary for the successful formation of endospores (4, 6). However, mature spores are deficient in MK but not in cytochromes, implying that MK deficiency may be a mechanism for inactivating the respiratory chain in dormant spores. Sporulation of *B. subtilis* is in part regulated by a form of catabolic repression that involves carbon- and/or nitrogen-containing metabolites (28, 30). Krebs cycle function is required for activation of the *spo0A* transcription factor in *B. subtilis* (14). However, *menp1* promoter activity has been shown to be independent of the presence of the products of the *spo0A* and *spo0H* genes and is enhanced in late stationary phase in culture medium containing glucose and glutamine (20).

When provided with a mixture of carbon sources, bacteria preferentially utilize those metabolized most readily, such as glucose. During glycolysis by *B. subtilis*, acidic and nonacidic end products such as acetate and acetoin are formed and subsequently secreted into the medium (Fig. 1A) (31), while energy production occurs principally by substrate level phosphorylation. Since *B. subtilis* does not reduce pyruvate to lactate or ethanol, it needs a functional respiratory chain at all times to regenerate NAD^+ for glycolysis. However, except for balancing reducing equivalents and providing short-chain carbon precursors for cellular synthesis, the tricarboxylic acid (TCA) cycle function is needed at a relatively low level during glycolysis; secondary carbon sources and glycolytic end products are not utilized until glucose is exhausted (8, 30). Excretion and extracellular accumulation of acidic and neutral compounds occur during glycolysis, leading to a low extracellular pH (31). When glucose is exhausted, oxidation of these end products depends on the uptake of the end products and their reutilization in the form of acetyl coenzyme A via the TCA cycle (Fig. 1A) (17, 18). At the oxidative metabolic stage, coordination of TCA cycle activity with the formation of respiratory chain components, especially MK, is essential for utilization of nonfermentable carbon sources.

* Corresponding author. Phone: (518) 473-2760. Fax: (518) 473-1326.

Most *B. subtilis* structural genes encoding biosynthesis of the naphthoquinone ring of MK have been isolated (3, 21, 26, 33). The enzymology of MK biosynthesis is understood, and gene-enzyme relationships have been established (3, 21, 23). In previous studies, *B. subtilis* genes encoding MK biosynthetic enzymes have been assigned to two major transcriptional units, the *menFD* and *menBE* operons (Fig. 2). Earlier physiological studies showed that biosynthesis of MK is growth phase dependent. In complex media, the cellular content of MK increases to a maximum at early stationary phase and declines rapidly to 1/10 of its maximum within 3 h (6). A similar kinetic profile of β-galactosidase activity was observed with *menp1-lacZ* (*menFD* operon) gene fusions (13, 20). These findings suggest that regulation of MK biosynthesis depends on transcriptional control of the *men* genes. Moreover, the gene fusion studies indicated that the elevated promoter activity in early stationary phase could be sustained into later stationary phase when the pH of the growth medium was lowered by acidification either through glycolysis or by external buffering at acidic pH (13). Thus, regulation of *menp1* appears to depend on both growth phase and environmental signals.

Here we report a transcriptional study of *menFD* gene expression in response to temporal and environmental changes. Bacterial culture conditions included various carbon sources, neutral and acidic pH buffering, and blockage of end product utilization pathways by mutation. In addition, the effects of promoter *cis* element mutagenesis on *men* transcription were determined.

MATERIALS AND METHODS

Bacterial strains and media. The *B. subtilis* strains and plasmids used in this study are listed in Table 1. RB1 (*trpC2*) is a derivative of the wild-type strain, *B. subtilis* 168, from which all cloned *men* material is derived. Growth supplements and antibiotics were obtained from Sigma Chemical Company, and media were obtained from Difco Laboratories. *B. subtilis* strains were maintained on Luria-Bertani (LB) medium. *B. subtilis* strains containing integrative plasmids conferring resistance to erythromycin, neomycin, or kanamycin were grown on LB agar plates containing 1 μg erythromycin per ml, 5 μg of neomycin per ml, or 10 μg kanamycin per ml, respectively. To test for integration of recombinant plasmids into the *B. subtilis amyE* locus (1, 29), amylase production was determined after growth on LB plates containing 1% soluble starch (United States Biochemical Corp.) by flooding the plates with 0.08 N I_2–0.32 N KI in 1% (wt/vol) sodium tetraborate. Promoter activity indicated by *lacZ* expression was detected by inoculating plates containing 4-methylumbelliferyl-β-D-galactoside (MUG) to identify fluorescent colonies under UV light.

For the study of *men* gene expression in response to various carbon sources, *B. subtilis* strains were grown in Schaeffer's sporulation medium containing no glucose; 0.1 or 0.5% glucose (13, 20), or 20 mM acetoin (Fluka), acetic acid

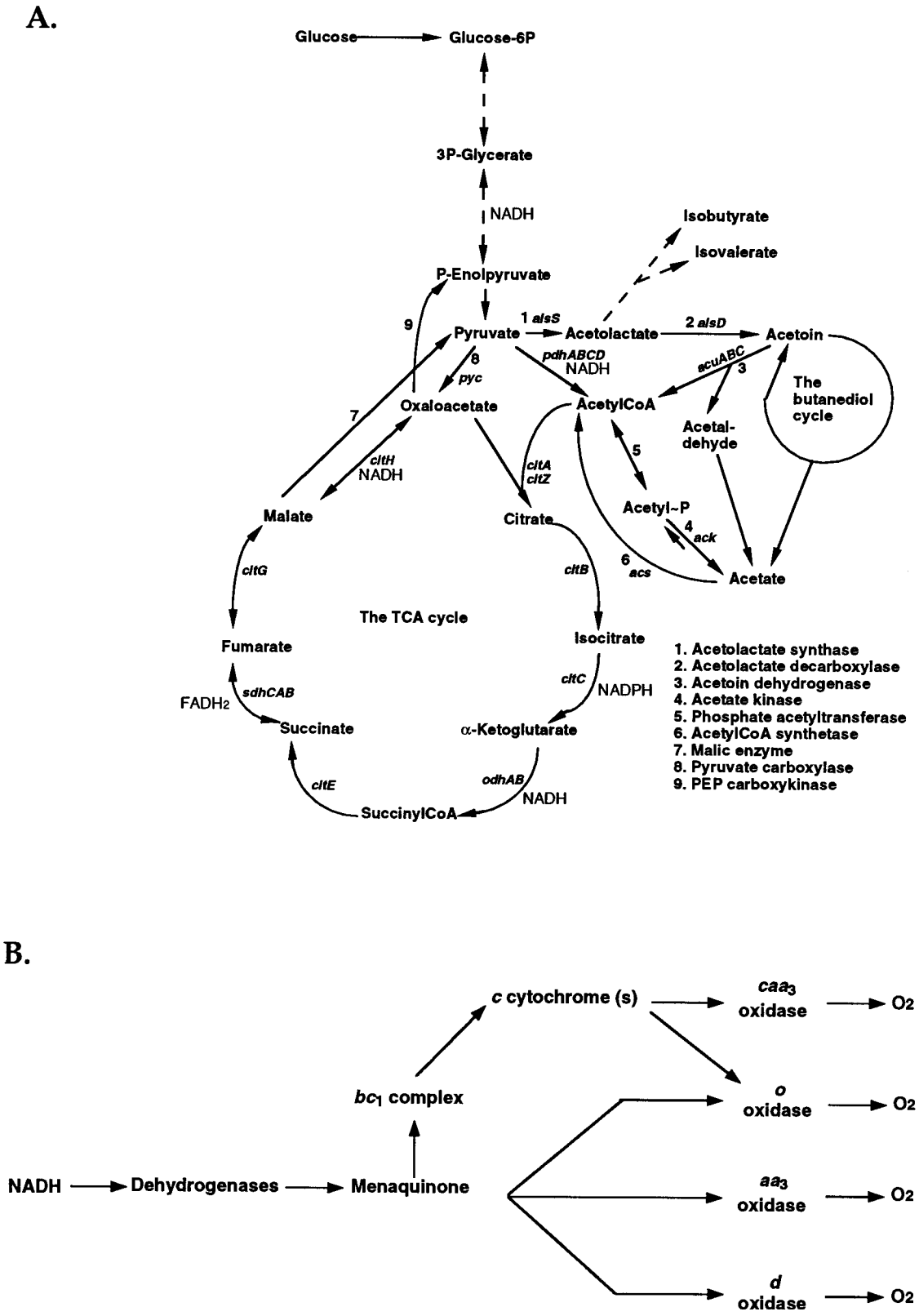

FIG. 1. (A) Biochemical pathways of carbon metabolism in *B. subtilis* (31). (B) *B. subtilis* respiratory chain. This diagram represents possible paths for aerobic electron transfer in bacilli (32).

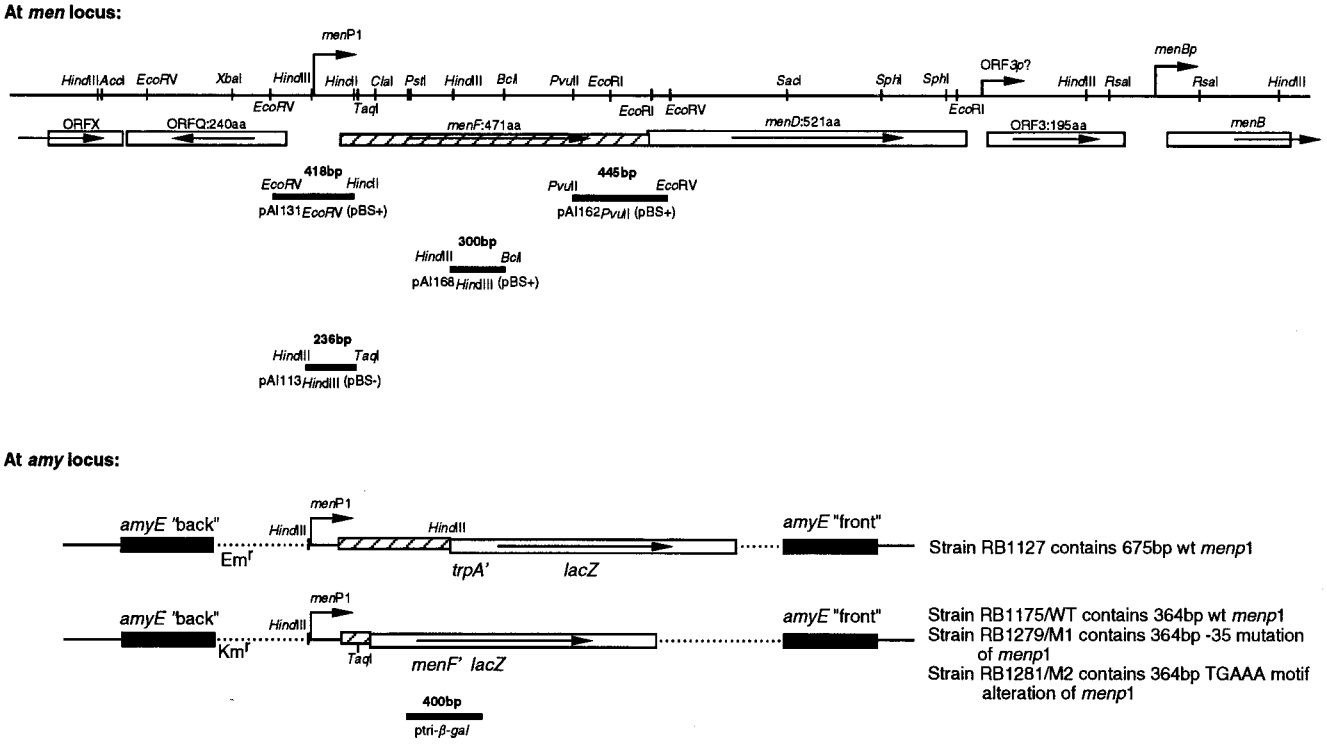

FIG. 2. Organization of *B. subtilis men* gene cluster and cRNA probes utilized for RPA of *menp1*-initiated mRNA at *men* and *amyE* loci of *B. subtilis* chromosome. Arrows indicate the positions of known promoters (3, 20). At *men* locus, the locations of the *menF*, *menD*, open reading frame 3 (ORF3), *menB*, and *menE* genes are indicated (3, 21, 26). Plasmids pAI113, pAI131, pAI162, and pAI168 are recombinant *men* gene constructs based on pBS+ and pBS−. Each plasmid was linearized by the enzyme indicated to generate templates ($pAI113_{HindIII}$, $pAI131_{EcoRV}$, $pAI162_{PvuII}$, or $pAI168_{HindIII}$) for synthesis of the cRNA probes. Genetic diagrams are shown for *B. subtilis* RB1127, RB1275, RB1281, and RB1283, indicating organization of the *menp1-lacZ* cassettes at the *amyE* locus. Hatched and open boxes indicate *men* genes, dotted lines indicate plasmid sequences, and black boxes indicate the bisected *amyE* gene. Em^r, erythromycin resistance gene; Km^r, kanamycin resistance gene. ptri-β-gal was purchased from Ambion in a linearized form. wt, wild type.

(Fisher Scientific), or malic acid (Sigma Chemical Co.). Stock solutions of acetate and malate were constructed such that they could be added to glucose-free Schaeffer's medium to produce a final pH of 5.5 and a 20 mM concentration of the respective acid.

For growth and pH measurements, *B. subtilis* strains were grown in Schaeffer's liquid medium containing various carbon sources. In some cases, Schaeffer's medium was buffered with 0.1 M MOPS [3-(*N*-morpholino)propanesulfonic acid; pH 7.0] or MES [2-(*N*-morpholino)ethanesulfonic acid; pH 5.5]. The medium (liquid-to-flask volume ratio of 1:10) was inoculated with cells to an initial A_{600} of approximately 0.02 as measured with a UV-visible spectrophotometer (Pharmacia). The flasks were shaken in a 37°C water bath at 250 rpm, and culture samples were taken every 0.5 to 1 h. The time points chosen for collection of cell samples were relative to time zero, which was defined as the point in the growth curve at which departure from exponential growth phase was first observed. The pH of the supernatant from the same sample was measured with a Cardy Twin pH meter kit (Horiba Instruments).

In vitro DNA manipulations, DNA sequencing, and bacterial cell transformation. Restriction digestions, ligations, small-scale isolation of plasmid DNA, and subclonings were performed by following either standard protocols (19) or the manufacturer's instructions for Magic Maxiprep or Wizard miniprep kits (Promega). All enzymes were obtained from three sources, United States Biochemical Corp., Sigma, and New England Biolabs. Double-stranded DNA was sequenced by the Sanger dideoxy chain-termination method with Sequenase version 2.0 (United States Biochemical Corp.) and [α-^{35}S]dATP (>1,000 Ci/mmol; Dupont) following the suppliers' protocols. Sequencing reaction products were resolved on 5% acrylamide (Long Ranger; J. T. Baker)–7 M urea gels. The complete sequences from both strands were determined. Chromosomal DNA was isolated from *B. subtilis* strains as described by Saunders et al. (27). *B. subtilis* was transformed by the method of Piggot et al. (24); *E. coli* was transformed by the method of Hanahan (12).

RNase protection assays. Isolation of total cellular RNA from *B. subtilis* was done with either the RNaid Plus kit (Bio 101, Inc.) or the RNeasy Total RNA kit (QIAGEN) following the supplier's protocol. Radioactive antisense RNA probes were generated by using the Ambion MAXIscript T7/T3 in vitro transcription kit following the supplier's protocol. [α-^{32}P]UTP (800 Ci/mmol) was obtained from Dupont. The full-length antisense RNA probes were isolated from polyacrylamide gels according to the supplier's instructions and hybridized to 5 to 10 μg of total cellular RNA. RNase protection assays were performed as described by Driscoll et al. (3), by using the RPA II kit (Ambion, Inc.). Quantification of the radioactivity in dried gels was carried out by using Storage PhosphorImaging (Molecular Dynamics). In these quantifications, the corresponding blank banding area in the yeast RNA control lane was chosen as the background 0 value. Volume readings above background were given in pixel values, which should quantitatively reflect the presence of the target messages for the same amount of total cellular RNA (10 μg) taken each 0.5 to 1 h throughout the growth cycle. The data presented in this study are averages of two to four independent experiments.

Site-directed mutagenesis by PCR. To generate site-directed mutations in *menp1* sequences, oligonucleotide XQM1 (55 nucleotides; 5′-AATTTAAGCTTTGTTTCTTGACAATTTCTGAAATTAGGTTTATAATAGGTAAGGC-3′) was made for the promoter −35 consensus mutation from TTTTTC to TTGACA (the underlined bases in XQM1), whereas oligonucleotide XQM2 (59 nucleotides; 5′-AATTTAAGCTTTGTTTCTTTTTCATTTCTCGAGTTAGGTTTATAATAGGTAAGGCAGGC-3′) was made for alteration of the sequence motif TGAAA to TCGAG (the underlined bases in XQM2). The primer for the corresponding wild-type control clone was XQF3 (25 nucleotides; 5′-CGGATACAACCTTTGCTATCAGTGG-3′), which annealed to a site upstream from the mutagenesis sites described above. The downstream PCR pairing primer was the oligonucleotide XQB12 (33 nucleotides; 5′-TGACAGGATCCAGAGGGTCAAGAGACTCGATTTGTC-3′), which was used in all cases. The template for these 264-bp PCR clones was pAI126. A set of three *menp1* variant clones was amplified by using the GeneAmp PCR Reagent Kit (Perkin-Elmer Cetus) with the Perkin Elmer DNA Thermal Cycler model 480. The PCR was carried out by following the supplier's standard protocol except that each PCR mixture contained 100 pmol of each primer and 20 ng of linearized plasmid template. The PCR products were digested with *Hin*dIII, filled in with a Klenow fragment, and then digested with *Bam*HI to give a uniform size of 270 bp. These fragments were cloned into the *Sma*I and *Bam*HI sites of pMD429 (a *B. subtilis amyE* integration vector [1]) resulting in a set of three *menp1-lacZ* translational fusion constructs. The gene fusion products were confirmed by sequencing with oligonucleotide LAC (5′-TGCAAGGCGATTAAGTTGG-3′).

Determination of acetoin, acetate, and malate concentrations. The Westerfeld modification of the Voges and Proskauer test was used for the colorimetric measurement of acetoin (35). A 0.5% aqueous creatine (Fluka) solution (0.2 ml)

TABLE 1. Bacterial strains and plasmids used in this study

Strains	Relevant genotype and phenotype	Source of Reference
Bacillus subtilis		
RB1	Marburg strain 168, *trpC2*	This laboratory
RB1127	RB1ΩpAI122, *trpC2* Em^r Lac^+ $AmyE^-$	This study
RB1271	ACSKO: *acs*::*neo* Nm^r	T. Henkin
RB1271	Acs^-, a Neo^r transformant of RB1 with DNA from ACSKO	This study
RB1275	WT, RB1ΩpAI170, *trpC2* Km^r Lac^+ $AmyE^-$	This study
RB1279	M1, RB1ΩpAI171, *trpC2* Km^r Lac^+ $AmyE^-$	This study
RB1281	M2, RB1ΩpAI172, *trpC2* Km^r Lac^+ $AmyE^-$	This study
RB1283	RB1ΩpMD429, *trpC2* Km^r Lac^- $AmyE^-$	This study
RB1285	ACUKO: *acu*::*neo* Nm^r	T. Henkin
RB1285	Acu^-, a Nm^r transformant of RB1 with DNA from ACUKO	This study
Escherichia coli		
JM107	*endA1 gyrA96 thi hsdR17 supE44 relA1* λ^- Δ(*lac-proAB*) [F′ *traD36 proAB* +*lacI*^{q} *lacZ* ΔM15] *mcrA*	*M. Belfort*
DH5α	F^- ϕ80d*lacZ*ΔM15 Δ(*lacZYA-argF*)*U169 deoR recA1 endA1 hsdR17* (r_K^- m_K^+) *supE44* λ^- *thi-1 gyrA96 relA1*	Bethesda Research Laboratories
Plasmids		
pAI113	pBS^- with a 236-bp *Hin*dIII-*Taq*I *menp1* fragment	This laboratory
pAI117	Amp^r Em^r; *amyE* integration vector	J. Mueller
pMD429	Amp^r Km^r; *amyE* integration vector	C. Meinhof
pAI122	pAI117 with a 675-bp *Hin*dIII *menp1* fragment	This study
pAI126	pSGMU2 with a 823-bp *Xba*I-*Pst*I *menp1* fragment	This study
pAI131	pBS^+ with a 1,189-bp *Hin*dIII-*Hin*cII *menp1* fragment	This study
pAI162	pBS^+ with a 1,015-bp *Hin*dIII-*Eco*RV *menFD* intercistronic fragment	This study
pAI168	pBS^+ with a 325-bp *Hin*dIII-*Bcl*I *menF* internal fragment	This study
pAI170	pMD429 with a 264-bp wt *menp1* fragment in frame fused to *lacZ*	This study
pAI171	pMD429 with a 264-bp *menp1*-M1 fragment in frame fused to *lacZ*	This study
pAI172	pMD429 with a 264-bp *menp1*-M2 fragment in frame fused to *lacZ*	This study
ptri-β-gal	Linearized plasmid for β-galactosidase antisense RNA probe synthesis	Ambion

and 5% α-naphthol (Fluka) (0.2 ml) in a 2.5 N NaOH solution were added to 1 ml of culture supernatant or diluted supernatant containing between 0.01 and 0.25 mM acetoin. The A_{540} was allowed to develop at room temperature for 60 min, at which time the color intensity was at its maximum. A standard curve relating acetoin concentration to A_{540} was constructed with an acetoin (Fluka) dilution series. Measurements of both acetate and malate were carried out by enzymatic assays based on NADH formation and were performed with assay kits purchased from Boehringer Mannheim following the supplier's standard protocols. Standard curves relating either the acetate or malate concentration to A_{340} were constructed with the dilution series by using standard substrates provided in the assay kits.

RESULTS

Genetic and transcriptional organization of *menFD* operon and mapping of *menp1*-initiated transcripts. Previous work has established that *menp1* (5′ proximal of *menF*) is the primary promoter for *menFD* operon expression (21). The mRNA initiation site of *menp1* (previously identified by S1 transcript mapping) (20) was confirmed by primer extension (data not shown). The protected fragments obtained in subsequent RNase protection assays (RPA) were consistent with the 5′ terminus determined by primer extension analysis. Antisense RNA probes generated from $pAI162_{PvuII}$ (Fig. 2) were also employed to identify polycistronic transcripts encompassing *menF* and *menD* initiated from *menp1* (data not shown).

Effects on *menp1*-initiated transcription of growth in pH-buffered and unbuffered media containing glucose. Total cellular RNA was isolated from the wild-type strain RB1 grown in Schaeffer's medium containing 0.1% glucose (condition I), 0.5% glucose (condition II), 0.1% glucose buffered at pH 7.0 with 0.1 M MOPS at inoculation (condition III), or 0.1% glucose buffered with 0.1 M MES to pH 5.5 at T_0 (to mimic the pH condition in cultures containing 0.5% glucose; condition IV). Antisense RNAs generated from $pAI113_{HindIII}$ and $pAI131_{EcoRV}$ (Fig. 2) were used to probe the RNA preparation for the 5′ part of *menp1*-initiated transcripts. A maximum level of *menp1* activity was seen from T_{-1} to T_1 for all four growth conditions (conditions I to IV) (Fig. 3A), and the specific responses of *menp1* in the post-exponential phase are shown by the sustained expression (to T_4) in 0.5% glucose-containing medium (condition II), as well as by either diminished (condition III, pH 7.0) or sustained expression (to T_2; condition IV, pH 5.5) in buffered media.

Quantification of four similar RPA (Fig. 3B) showed that the *menp1*-initiated transcript accumulation was maximal in exponential phase (T_{-1}) and at T_0 to T_1. The level of *menp1* transcripts then declined rapidly when cells were grown in medium containing low levels of glucose (0.1%). However, in medium containing high levels of glucose (0.5%), the maximal *menp1* activity was sustained throughout exponential and post-exponential phases (T_{-1} through T_4) (Fig. 3B). In the same experiments, extracellular pH measurements were made during the culture cycle. These measurements indicated that transient acidification occurred at T_0 to T_1 during growth in Schaeffer's medium containing 0.1% glucose. However, growth in 0.5% glucose-containing medium resulted in sustained acidification throughout the period T_0 to T_4 (Fig. 3C).

In agreement with previous *menp1-lacZ* genetic fusion studies by Hill et al. (13), *menp1* activity during the post-exponential phase was sustained through stage T_2 with a low level of glucose (0.1%) when the culture medium was buffered to pH 5.5 at T_0 (Fig. 3B). On the other hand, post-exponential-phase *menp1* transcription was entirely eliminated when the culture medium was buffered to pH 7.0 at the time of inoculation (Fig.

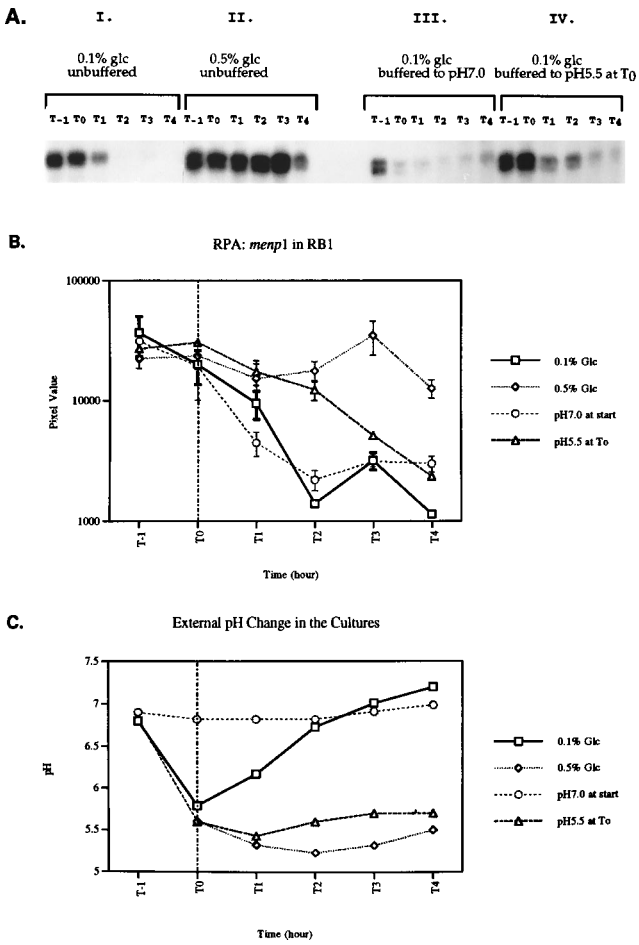

FIG. 3. (A) RPA autoradiograph of *menp1*-initiated mRNA isolated from strain RB1, utilizing cRNA probes generated from pAI131$_{EcoRV}$ (Fig. 2). Strain RB1 was grown in Schaeffer's medium with the carbon source and pH conditions indicated below the group designations, I, II, III, and IV. RPA was performed with a 441-nucleotide cRNA probe, pAI131$_{EcoRV}$; 418 nucleotides were specific to the *menp1-menF'* region, and 23 nucleotides were nonspecific. The ^{32}P-labelled probe (2×10^5 cpm) was hybridized with 10 μg of RNA isolated from RB1 cultures harvested at the times indicated above each lane and digested with a combination of RNase A and T_1 as described in Materials and Methods; yeast RNA controls and full-length probes are not shown. glc, glucose. (B) Average quantification results from four repeats of the experiment described for panel A. Average pixel values were graphed against time T_{-1} to T_4 as indicated. Quantitative deviations of pixel values generated from independent experiments are indicated by the error bars (note: depending on the size of the plot frame, the axis scale, and error value, some error bars do not appear in the graph because they are relatively too small). (C) External pH change in different cultures as indicated. The different culture conditions correspond to groups I to IV in panel A.

3B). This result seemed to suggest that *menp1* is pH regulated. Alternatively, acidic pH (pH 5.5) may facilitate the diffusion of acidic carbon sources (or acidic glycolysis end products) in their protonated forms into the cells, which in turn stimulates *men* expression.

Effects of growth in nonfermentable carbon sources on *menp1*-initiated transcription. The addition of individual secondary carbon sources to the culture medium was used to mimic the presence of glycolytic end products. Cultures were grown to stage T_0 in glucose-free Schaeffer's medium, and then one of the nonfermentable carbon sources (acetoin, acetate, or malate [Fig. 1A]) was added to a concentration of 20 mM. The pH of the medium was carefully controlled and monitored, and no changes in growth were observed following the addition of the carbon source. Acetoin is a nonacidic end product which does not acidify the growth medium, but acetate and malate are carboxylic acids. Stock solutions of the latter compounds had to be adjusted so that the pH of the growth medium after the addition would be approximately pH 5.5 (see Materials and Methods) to mimic the pH value at T_0 in cultures containing 0.5% glucose (Fig. 3C). The *B. subtilis* strain used was RB1127 (*amyE*::*menp1-lacZ* [Fig. 2]). The purpose of utilizing this strain was twofold. First, it assisted in identifying a DNA sequence segment sufficient in length to contain all of the elements for *menp1* wild-type activity. This was done by employing multiprobe RPA using antisense RNA probes generated from the plasmids pAI168$_{HindIII}$ and ptri-β-gal (Ambion) (Fig. 2 and Table 1), in which *menp1*-initiated transcripts at the native locus served as positive internal controls for the activity of *menp1* at the *amyE* locus (Fig. 2). Secondly, the *menp1-lacZ* cassette at *amyE* served for later efforts to mutagenize *menp1.*

Responses of *menp1* to secondary carbon sources were reflected in transcript accumulation (Fig. 4A). The kinetics of these responses in the post-exponential phase (Fig. 4B and C) was correlated with the loss of the corresponding carbon compounds from the culture supernatants (Fig. 4D) and with a pH change (Fig. 4E). Consistent with previous results in 0.1% glucose-containing medium, *menp1*-initiated transcripts reached maximal values during the period T_{-1} to $T_{0.5}$ and then declined rapidly to a very low level after T_1 (Fig. 4A, conditions I to IV). However, if any one of the three nonfermentable carbon sources (acetoin, acetate, or malate) was provided, the specific *menp1*-initiated mRNA level could be reelevated in the late post-exponential-phase period T_3 to T_4 (Fig. 4A, II, III, and IV, and 4B and C). The decline in transcript level at T_1 in the presence of malate was blunted (Fig. 4B and C), probably because of rapid uptake and utilization of this carbon source (Fig. 4D). Measurements of *menp1* activity by multiprobe RPA suggested similar expression kinetics of *menp1* at the two loci in various carbon and pH conditions, although the steady-state levels of the two transcripts differed (Fig. 4B and C). This result also confirms that the 675-bp *Hin*dIII fragment at *amyE* contains sufficient sequences to support wild-type *menp1* activity.

Effects on *menp1* activation of introducing mutations blocking pathways for glycolytic end product utilization. Mutations in two genes, *acuA* (acetoin utilization) and *acsA* (encoding acetyl coenzyme A synthetase; acetate utilization) encoding end product-utilizing enzymes, induce metabolic disturbances that prevent acetoin or acetate from entering the TCA cycle via acetyl coenzyme A (Fig. 1A) (10, 11). Strains RB1285a (Acu$^-$) and RB1271a (Acs$^-$) were grown in glucose-free Schaeffer's medium with and without the addition of acetoin and acetate, respectively. Transcripts initiated from *menp1* at the native locus were measured by hybridization with antisense RNA generated from pAI113$_{HindIII}$ (Fig. 2).

Monitoring of the extracellular concentration of acetoin or acetate during the culture cycle demonstrated the expected biochemical deficiencies in Acu$^-$ or Acs$^-$ strains and the prominent functions of the *acu-* or *acs*-encoded enzymes (data not shown). RPA measurements showed that the post-exponential-phase reelevation of *menp1*-initiated transcripts in response to the addition of acetoin or acetate at T_0, characteristic of the wild-type strain RB1, was totally abolished in either Acu$^-$ or Acs$^-$ strains (Fig. 5) (quantification of typical results is shown beneath the autoradiographs). In the two growth conditions for strain Acu$^-$ described above (i.e., with or without the addition of acetoin at T_0), the level of *menp1* activity remained very low from T_2 through T_4 (Fig. 5A, conditions II

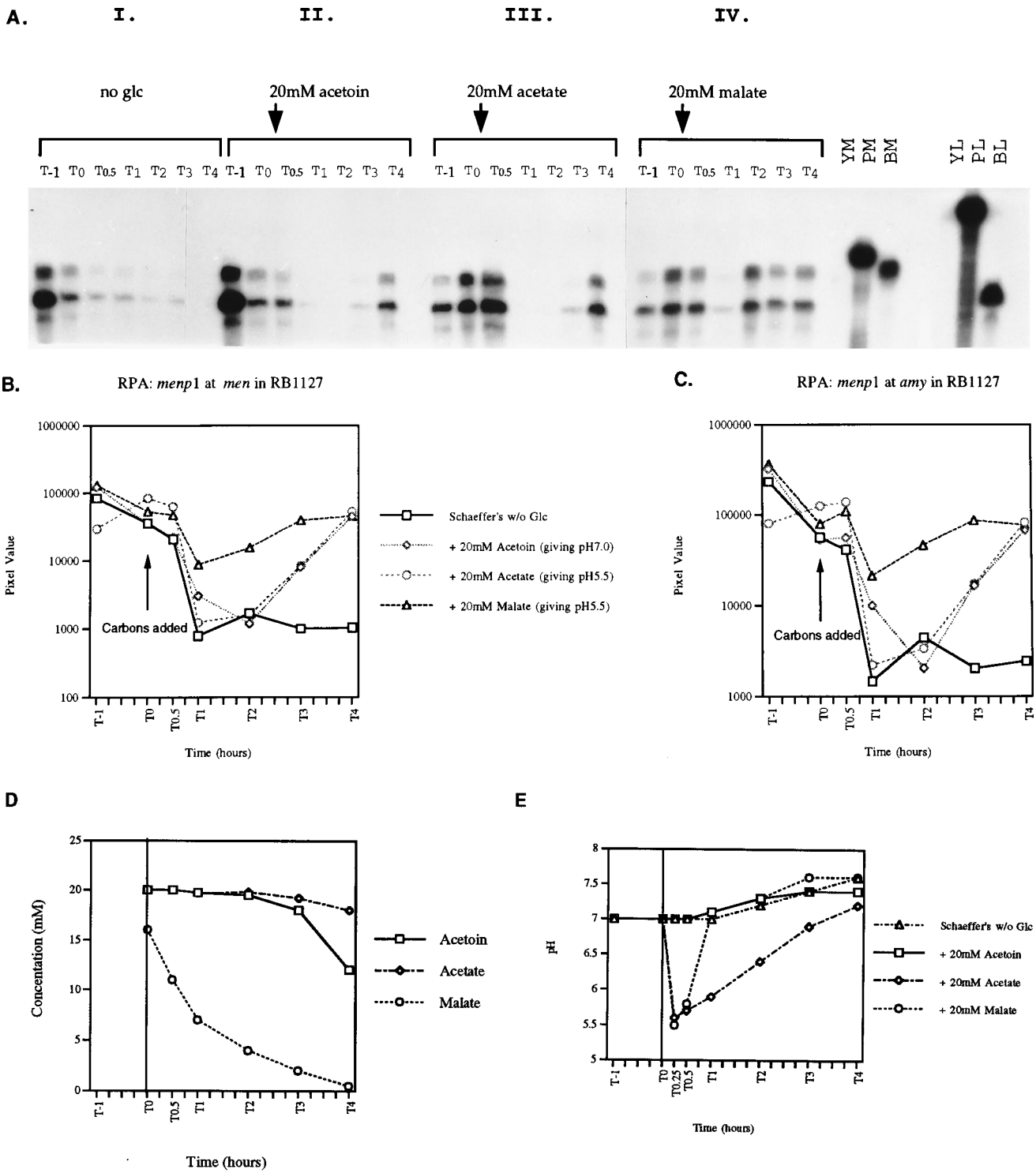

FIG. 4. (A) RPA autoradiograph of *menp1*-initiated mRNA isolated from strain RB1127, with a multiprobe assay (pAI168$_{HindIII}$ and ptri-β-gal). Strain RB1127 was grown in unbuffered Schaeffer's medium with carbon sources indicated below groups I to IV. As shown in Fig. 2, pAI168$_{HindIII}$ yields a 309-nucleotide cRNA, 300 nucleotides of which are specific to a *menF* internal region and 9 nucleotides of which are nonspecific; ptri-β-gal yields a 400-nucleotide cRNA, 283 nucleotides of which are specific to a *lacZ* internal region and 117 nucleotides of which were nonspecific. The ^{32}P-labelled probes (2×10^5 cpm) were hybridized with 10 μg of RNA isolated from strain RB1127 harvested at the times indicated above each lane and digested with a combination of RNase A and T_1 as described in Materials and Methods. Lanes BM and BL, 2×10^5 cpm of pAI168$_{HindIII}$ and ptri-β-gal, respectively, hybridized to 10 μg of RB1127 RNA and treated with RNase; lanes YM and YL, 2×10^5 cpm of pAI168$_{HindIII}$ and ptri-β-gal, respectively, hybridized to 10 μg of yeast RNA and treated with RNase; lanes PM and PL, 2×10^5 cpm of pAI168$_{HindIII}$ and ptri-β-gal alone, respectively, hybridized to 10 μg of yeast RNA not treated with RNase. The arrows indicate the time at which carbon sources were added to the cultures. (B and C) Average quantification results from four repeats of RPA (panel A). Average pixel values were graphed against time as indicated for *menp1*-initiated transcripts from two independent loci (quantitative deviations of pixel values generated from independent experiments were too small to be shown); measurements of *menp1*-initiated mRNA at *men* by pAI168$_{HindIII}$ (B) and at *amyE* by ptri-β-gal (C) are shown. The arrows indicate the time at which carbon sources were added to the cultures. (D) Acetoin, acetate, and malate utilization in strain RB1127. Carbon sources were added at T_0, and measurements of acetoin, acetate, and malate concentrations in the supernatant were made hourly until T_4. The concentrations of the respective carbon compounds were graphed against the time course from which the cell samples (for RPA as described for panel A) and supernatant samples were collected. Degradation controls for the three carbon compounds were monitored by incubating filter-sterilized supernatant from a culture of RB1127 (grown to T_0) with each of the respective compounds. The concentration of each substrate was stable through T_4 (data not shown). (E) External pH change in the cultures of strain RB1127 in Schaeffer's medium containing various carbon sources. Glc, glucose.

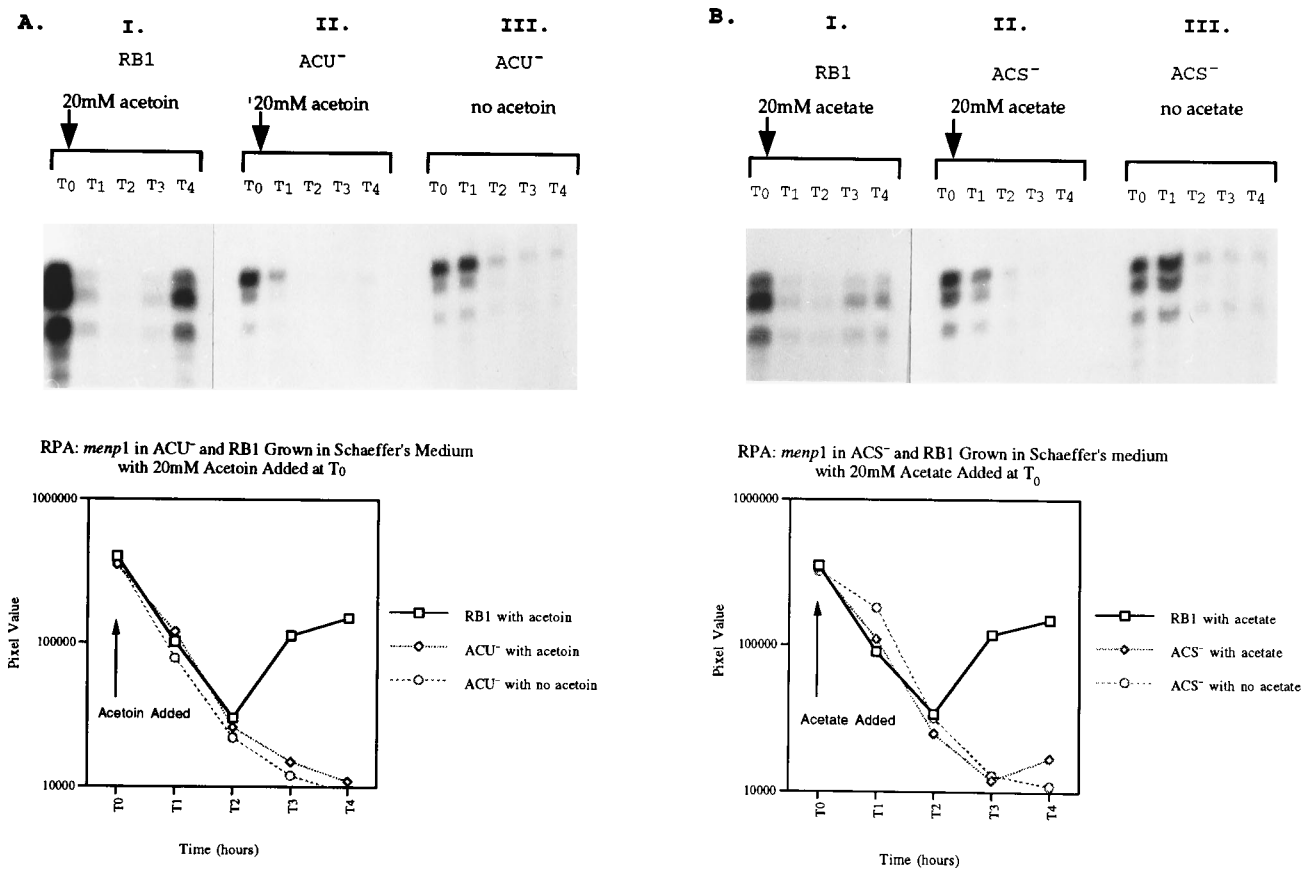

FIG. 5. RPA of *menp1*-initiated mRNA isolated from strains Acu$^-$ (RB1285a) and RB1 grown in Schaeffer's medium with addition of acetoin at T_0 (A) from strains Acs$^-$ (RB1271a) and RB1 grown in Schaeffer's medium with addition of acetate at T_0 (B). *B. subtilis* strains and their growth media are indicated below each group. The arrow indicates the times at which carbon sources were added to the cultures. RPA was performed with an antisense RNA probe derived from pAI113$_{HindIII}$ (Fig. 2). The ^{32}P-labelled probe (2×10^5 cpm) was hybridized with 10 μg of RNA isolated from strains Acu$^-$, Acs$^-$, or RB1 harvested at the time indicated above each lane and digested with a combination of RNase A and T_1 as described in Materials and Methods; the results for the yeast RNA control and full-length probe are not shown. Average quantification results for the respective strains are shown below the autoradiographs.

and III). Likewise, for the two growth conditions for strain Acs$^-$ described above (with or without the addition of acetate at T_0), the level of *menp1* activity remained very low from T_2 through T_4 (Fig. 5B, conditions II and III). Loss of *menp1* activity reelevation in Acu$^-$ and Acs$^-$ mutants in response to the respective substrates (acetoin or acetate) suggested involvement (in the wild-type strain RB1) of an internal inducer molecule generated by the utilization of either acetoin or acetate.

Mutagenesis of *menp1* regulatory motif TGAAA. A previously described regulatory sequence motif, TGAAA, occurring between the −35 and −10 regions of *menp1* (3), together with its palindromic half in the −35 region (TTTTTCA), was targeted for site-specific mutagenesis to determine the effects on *menp1* activity. Two types of sequence alterations were created by PCR mutagenesis: (i) a mutation (M1) to create a σ^A-type −35 consensus sequence by altering TTTTTCA to TTGACAA and (ii) a mutation (M2) of the TGAAA sequence in the −35/−10 spacer region of *menp1* by altering (C)TGAAA to (C)TCGAG (the *Xho*I restriction site was created to facilitate promoter spacing alterations). These two sequence alterations are illustrated in Fig. 6. The altered M1- and M2-*menp1* clones (recombinant plasmids pAI171 and pAI172, respectively) together with the wild-type clone (pAI170) were constructed in the *amyE* integrative *lacZ* translational fusion vector pMD429 (Table 1) as described in Materials and Methods. The *B. subtilis* transformants generated were strains RB1275 for the wild type, RB1279 for M1, and RB1281 for M2 (Table 1 and Fig. 2). The genetic linkage between AmyE$^-$ and Km^r Lac$^+$ was 100% in all RB1 transformants (strains RB1275, RB1279, and RB1281). The three *menp1-lacZ* fusion products were analyzed by RPA with the antisense RNA probe ptri-β-gal (Fig. 2). Carbon sources for the growth conditions utilized as described above were also used.

As expected, alteration of the −35 sequence of *menp1* to match consensus created a promoter ~20 times stronger than the wild type as indicated by a >20-fold increase in *menp1*-initiated transcripts throughout the growth cycle in glucose-free medium (Fig. 7). The intensity of the signal corresponding to the protected transcripts (when M1 and the wild type were compared) differed proportionally in the corresponding five samples from either of the two strains (T_0 through T_4 for conditions I and II in Fig. 7A and RPA quantification in Fig. 7B). This suggests that creation of a perfect −35 consensus sequence (as in M1) does not cause a change in the regulation of *menp1* expression but results only in an increase of promoter strength. However, alteration of the (C)TGAAA motif in the promoter region (as in M2) did not change the promoter strength but caused loss of regulation during the post-exponential period (condition III in Fig. 7A and quantification in

```
HindIII
|             M1        M2                                                    100
|           TTGACA    CTCGAG                  *                               *
AAGCTTTGTTTCTTTTTCATTTCTGAAATTAGGTTTATAATAGGTAAGGCAGGCCATTTGGACTGCATGATCTGTGTTTGACACAAAGGAGACACAGGTG
              -35                    -10       +1

                                        *
TATGGTATTAAAAGCATTTTAAGGATTATGGAGGAATGTCTC ATG GTG ACA ACG GTG CAG CGT ACG TTC CGA AAG GAA GTT CTA CAT
                              rbs          menF start

               200          HincII                          TaqI
                *             |                              |
GCA TTA CAT AAA GCC AAA GAA GTC AAC CAT GCT GTC TTA ATA AGC TAT TCG AGA CAA ATC GAG TCT CTT GAC CCT

   BamHI
264|          EcoRI
  *|           |                lacZ
 CTG GAT CCG GGG AAT TCA-------------------------
```

FIG. 6. Site-directed mutagenesis of putative regulatory sequences in *menp1* promoter region. The 264-bp DNA sequences are the PCR mutagenesis products of *menp1* fused in frame to the seventh codon of *lacZ*. The wild-type −35 and −10 promoter consensus sequence of *menp1* and the ribosomal binding site for *menF* translation are underlined. M1 and M2 (indicated by nucleotides above the wild-type sequences) are the two changes made to the palindromic sequences (bold letters). The relevant restriction enzyme sites are indicated.

Fig. 7B). This loss of regulation occurred regardless of the carbon sources added at T_0 (data not shown).

DISCUSSION

Nonfermentable carbon sources appear to serve as positive signals for *menp1* promoter activation in the post-exponential phase. When cells are grown in the presence of a fermentable carbon source such as glucose, the accumulated glycolytic end products provide signals for *menp1* activation in late post-exponential phase (0.5% glucose, condition II [Fig. 3A]). These compounds appear to serve to coordinate activation of the TCA cycle and formation of the respiratory chain. Buffering of the growth medium to lower the extracellular pH may facilitate the uptake of acidic end products, and this may contribute to the apparent regulatory effect of low pH. However, the neutral carbon compound acetoin mediates the same positive activation effect on *menp1* expression without acidifying the culture medium (condition II in Fig. 4A and E). This result suggests that the carbon compounds themselves, perhaps in addition to acidic pH, provide the signal for *menp1* transcription.

Studies with *acuABC* and *acsA* mutants indicate the existence of an internal inducer molecule for *menp1* activation, derived from the utilization of glycolytic end products. Citrate, the first intermediate in the TCA cycle, is considered to be the inducer molecule for *citB* transcription (9, 30) and subsequently activates other TCA cycle genes. However, *citB* and *men* differ on the basis of their responses to glutamine. While glutamine with glucose confers an added repression effect on *citB* (2, 7, 9, 25), glutamine by itself can activate *menp1* (20). Furthermore, in contrast to TCA cycle activity, MK formation is not repressed during glycolysis. Therefore, it is likely that the molecular mechanisms of activation of the TCA cycle and respiratory chain differ but are coordinated. If an inducer molecule exists for *menp1* activation, it must be a molecule that can be derived from the activities of both glycolysis and the TCA cycle. To fulfill these requirements, the inducer might well be the carrier of reducing equivalents, NADH.

The temporal activation of *menp1* during rapid growth (in exponential and early post-exponential phases) supports the possibility that NADH might be an inducer for the formation of MK. The need for an active electron transport chain for oxidation of NADH formed during rapid growth in complex

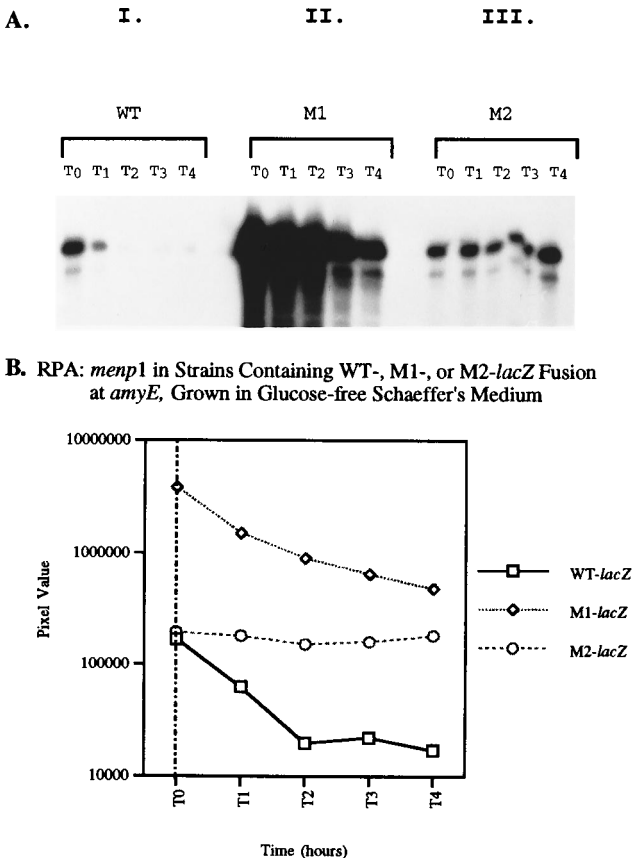

FIG. 7. (A) RPA autoradiograph of *menp1*-initiated mRNA isolated from strains M1 (RB1279), M2 (RB1281), and wild type (WT) (RB1275). Each strain contains a copy of a *menp1-lacZ* fusion located at *amyE* (Fig. 2). The strains were grown in unbuffered Schaeffer's medium without glucose and grouped in I, II, and III (from left to right) as indicated. RPA was performed with the cRNA probe ptri-β-gal shown in Fig. 2. The ^{32}P-labelled probe (2×10^5 cpm) was hybridized with 5 μg of RNA isolated from the respective three strains harvested at the times indicated above each lane and digested with a combination of RNase A and T_1 as described in Materials and Methods; the results for the yeast RNA control and full-length probe are not shown. (B) Average quantification results for two RPA as described for panel A. Average pixel values were graphed against time as indicated.

medium or glucose-containing medium is indicated by the presence of high concentrations of both MK and the quinol oxidases cytochrome aa_3 and *o* in exponential and early post-exponential phases (6, 15, 16). In late post-exponential-growth phase, *menp1* activity can be sustained by the addition of carbon sources other than glucose or otherwise can be inactivated or repressed because of the exhaustion of carbon sources. In both situations, the cellular concentration of NADH could serve as a measure of carbon availability. Direct measurements of intracellular NADH would test this hypothesis. These responses of *menp1* are similar to those observed for transcription of *ctaA* (22) and for accumulation of caa_3 oxidase (16).

The poor match to consensus (two of six) in the −35 region of *menp1*, together with the perfect match (six of six) in the −10 region, suggests that *menp1* is a good candidate to be a highly regulated promoter. The −35 consensus mutation increased promoter strength so substantially that any fluctuation in promoter activity initiated by environmental signals, if it still existed, was impossible to detect. To study such regulatory mechanisms for *menp1* in the future, it will be necessary to design mutations that will not change promoter strength but confer alterations only in the carbon source- and growth-phase-dependent kinetics of *menp1*. In a search for regulatory sites within *menp1*, the TGAAA motif was targeted because of the frequency with which it appears in promoter regions of genes encoding oxidative functions in *B. subtilis* (3). Alteration of the TGAAA motif within *menp1* had a striking effect in creating unregulated expression of *menp1* throughout the culture cycle regardless of carbon source availability. Thus, this sequence may be a site at which a factor acts to reduce *menp1* activity in the absence of glycolytic end products and other nonfermentable carbon sources. The response of *menp1* to external nonfermentable carbon sources in late stationary phase might be channeled through a derepression mechanism. Thus, the TGAAA motif during hypothesized to play an important role in regulation during post-exponential phase. To study such mechanisms, it would be helpful to place a mutated TGAAA at the native *men* locus; it may then be possible to isolate suppressors in this mutant background that are altered in effectors modifying *menp1* activity.

ACKNOWLEDGMENTS

We thank T. Henkin for providing strains and discussion, M. Dahl and D. Zeigler of BGSC for providing strains, A. Arrow of Oligo's etc. and the Wadsworth Center Molecular Genetics Core for providing oligonucleotides, and B. Rowland, J. Driscoll, C. Lowry, M. Wolin, J. Salvo, and M. Belfort for helpful discussions.

This investigation was supported in part by a grant from the National Institutes of Health (GM44547).

REFERENCES

1. **Dahl, M. K., and C.-G. Meinhof.** 1994. A series of integrative plasmids for *Bacillus subtilis* containing unique cloning sites in all three open reading frames for translational *lacZ* fusions. Gene **145:**151–152.
2. **Dingman, D. W., M. S. Rosenkrantz, and A. L. Sonenshein.** 1987. Relationship between aconitase gene expression and sporulation in *Bacillus subtilis*. J. Bacteriol. **169:**3068–3075.
3. **Driscoll, J. R., and H. W. Taber.** 1992. Sequence organization and regulation of the *Bacillus subtilis menBE* operon. J. Bacteriol. **174:**5062–5071.
4. **Escamilla, J. E., B. Baguera, R. Ramirez, A. Garcia-Horsman, and P. del Arenal.** 1988. Role of menaquinone in inactivation and activation of the *Bacillus cereus* forespore respiratory system. J. Bacteriol. **170:**5908–5912.
5. **Farrand, S., and H. Taber.** 1973. Physiological effects of menaquinone concentration during growth and early sporulation in *Bacillus subtilis*. J. Bacteriol. **117:**324–326.
6. **Farrand, S., and H. Taber.** 1974. Changes in menaquinone concentration during growth and early sporulation in *Bacillus subtilis*. J. Bacteriol. **117:**324–326.
7. **Fisher, S. H., and B. Magasanik.** 1984. 2-Ketoglutarate and the regulation of aconitase and histidase formation in *Bacillus subtilis*. J. Bacteriol. **159:**379–382.
8. **Fisher, S. H., and A. L. Sonenshein.** 1991. Control of carbon and nitrogen metabolism in *Bacillus subtilis*. Annu. Rev. Microbiol. **45:**107–1035.
9. **Fouet, A., and A. L. Sonenshein.** 1990. A target for carbon source-dependent negative regulation of the *citB* promoter of *Bacillus subtilis*. J. Bacteriol. **172:**835–844.
10. **Grundy, F. J., A. J. Turinsky, and T. M. Henkin.** 1994. Catabolite regulation of *Bacillus subtilis* acetate and acetoin utilization genes by CcpA. J. Bacteriol. **176:**4527–4533.
11. **Grundy, F. J., D. A. Waters, T. Y. Takova, and T. M. Henkin.** 1993. Identification of genes involved in utilization of acetate and acetoin in *Bacillus subtilis*. Mol. Microbiol. **10:**2959–2971.
12. **Hanahan, D.** 1985. Techniques for transformation of *E. coli*. p. 1–17. *In* D. M. Glover (ed.), DNA cloning, vol. I. A Practical Approach. Oxford, IRL Press.
13. **Hill, K. F., J. Mueller, and H. Taber.** 1990. The *Bacillus subtilis menCD* promoter is responsive to extracellular pH. Arch. Microbiol. **153:**355–359.
14. **Ireton, K., S. Jin, A. D. Grossman, and A. L. Sonenshein.** 1995. Krebs cycle function is required for activation of the Spo0A transcription factor in *Bacillus subtilis*. Proc. Natl. Acad. Sci. USA **92:**2845–2849.
15. **Lauraeus, M., T. Haltia, M. Saraste, and M. Wikström.** 1991. *Bacillus subtilis* expresses two kind of heme A-containing terminal oxidases. Eur. J. Biochem. **197:**699–705.
16. **Lemma, E., J. Simon, H. Schägger, and A. Kröger.** 1995. Properties of the menaquinol oxidase (Qox) and of *qox* deletion mutants of *Bacillus subtilis*. Arch. Microbiol. **163:**432–438.
17. **Lopez, J. M., and P. Fortnagel.** 1972. The regulation of the butanediol cycle in *Bacillus subtilis*. Biochim. Biophys. Acta **279:**544–560.
18. **Lopez, J. M., B. Thomas, and H. Rehbein.** 1975. Acetoin degradation in *Bacillus subtilis* by direct oxidative cleavage. Eur. J. Biochem. **57:**425–430.
19. **Maniatis, T., E. F. Fritsch, and J. Sambrook.** 1982. Molecular cloning: a laboratory manual. Cold Spring Harbor Laboratory, Cold Spring Harbor, N.Y.
20. **Miller, P., J. Mueller, K. Hill, and H. Taber.** 1988. Transcriptional regulation of a promoter in the *men* gene cluster of *Bacillus subtilis*. J. Bacteriol. **170:**2742–2748.
21. **Miller, P., A. Rabinowitz, and H. Taber.** 1988. Molecular cloning and preliminary genetic analysis of the *men* gene cluster of *Bacillus subtilis*. J. Bacteriol. **170:**2735–2741.
22. **Mueller, J. P., and H. W. Taber.** 1989. Structure and expression of the cytochrome aa_3 regulatory gene *ctaA* of *Bacillus subtilis*. J. Bacteriol. **171:** 4979–4986.
23. **Palaniappan, C., H. Taber, and R. Megnathan.** 1994. Biosynthesis of *o*-succinylbenzoic acid in *Bacillus subtilis*: identification of *menD* mutants and evidence against the involvement of the α-ketoglutarate dehydrogenase complex. J. Bacteriol. **176:**2648–2653.
24. **Piggot, P. J., C. A. M. Curtis, and H. deLancastre.** 1984. Demonstration of a polycistronic transcription unit required for sporulation of *Bacillus subtilis* by use of integrational plasmid vectors. J. Gen. Microbiol. **130:**2123–2136.
25. **Rosenkrantz, M. S., D. W. Dingman, and A. L. Sonenshein.** 1985. *Bacillus subtilis citB* gene is regulated synergistically by glucose and glutamine. J. Bacteriol. **164:**155–164.
26. **Rowland, B. M., K. Hill, P. Miller, J. Driscoll, and H. W. Taber.** 1995. Structural organization of a *Bacillus subtilis* operon encoding menaquinone biosynthetic enzymes. Gene **167:**105–109.
27. **Saunders, C. W., B. J. Schmidt, M. S. Mirot, L. D. Thompson, and M. S. Guyer.** 1984. Use of chromosomal integration in the establishment and expression of *blaZ*, a *Staphylococcus aureus* β-lactamase gene, in *Bacillus subtilis*. J. Biol. Chem. **157:**718–726.
28. **Schaeffer, P., J. Millet, and J.-P. Aubert.** 1965. Catabolite repression of bacterial sporulation. Proc. Natl. Acad. Sci. USA **54:**704–711.
29. **Shimotsu, H., and D. J. Henner.** 1986. Construction of a single-copy integration vector and its use in analysis of regulation of *trp* operon of *Bacillus subtilis*. Gene **43:**85–94.
30. **Sonenshein, A. L.** 1989. Metabolic regulation of sporulation and other stationary-phase phenomena, p. 109–130. *In* I. Smith, R. A. Slepecky, and P. Setlow (ed.), Regulation of procaryotic development. American Society for Microbiology, Washington, D.C.
31. **Speck, E. L., and E. Freese.** 1973. Control of metabolite secretion in *Bacillus subtilis*. J. Gen. Microbiol. **78:**261–275.
32. **Taber, H. W.** 1993. Respiratory chains, p. 199–212. *In* A. L. Sonenshein, J. A. Hoch, and R. Losick (ed.), *Bacillus subtilis* and other gram-positive bacteria. American Society for Microbiology, Washington, D.C.
33. **Taber, H. W., E. A. Dellers, and L. R. Lombardo.** 1981. Menaquinone biosynthesis in *Bacillus subtilis*: isolation of *men* mutants and evidence for clustering of *men* genes. J. Bacteriol. **145:**321–327.
34. **Taber, H. W., and E. Freese.** 1974. Sporulation properties of cytochrome *a*-deficient mutants of *Bacillus subtilis*. J. Bacteriol. **120:**1004–1011.
35. **Westerfeld, W. W.** 1945. A colorimetric determination of blood acetoin. J. Biol. Chem. **161:**495–502.